

Beyond electronics, beyond optics: single circuit parallel computing with phonons

Sophia Sklan¹ and Jeffrey C. Grossman²

¹*Department of Physics, Massachusetts Institute of Technology, Cambridge, Massachusetts, 02139, United States.*

²*Department of Materials Science and Engineering, Massachusetts Institute of Technology, Cambridge, Massachusetts, 02139, United States.*

Phononic computing – the use of (typically thermal) vibrations for information processing – is a nascent technology; its capabilities are still being discovered. We analyze an alternative form of phononic computing inspired by optical, rather than electronic, computing. Using the acoustic Faraday effect, we design a phonon gyrator and thereby a means of performing computation through the manipulation of polarization in transverse phonon currents. Moreover, we establish that our gyrators act as generalized transistors and can construct digital logic gates. Exploiting the wave nature of phonons and the similarity of our logic gates, we demonstrate parallel computation within a single circuit, an effect presently unique to phonons. Finally, a generic method of designing these parallel circuits is introduced and used to analyze the feasibility of magneto-acoustic materials in realizing these circuits.

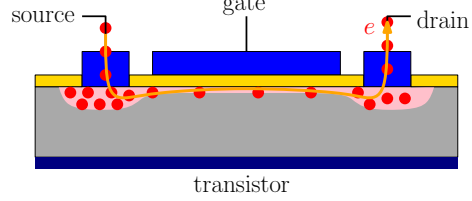
PACS numbers: 85.70.Ec, 63.20.kk, 72.55.+s, 43.25.-x

Computers are unquestionably useful, thanks in no small part to their silicon-based electronic architecture. After all, the size and expense of vacuum tube computers rendered personal computing impossible. Today, there are many proposed alternatives to silicon computers. Quantum computing, for example, promises to perform calculations more efficiently than any classical computer could [1]. Moreover, biological and fuzzy logic computers outperform classical computers in specific applications but are unlikely to supplant traditional computers [2, 3]. The creation of phonon (vibrational) equivalents of electronic computer elements has recently been explored. Phononic (often called thermal) computing's typical application is to use heat from electronic computers, where waste heat is cheap, plentiful, and wasted [4, 5].

The development of further applications for phonon computers has been stymied by the difficulty in controlling phonon propagation. This is aggravated by reliance upon analogies between temperature and voltage, thus taking inspiration from electronics [4–8]. Such focus has yielded reliance upon nanostructured materials [9, 10] and 1D, nonlinear chains [4–6, 11] to construct circuit elements. While this has resulted in difficulties with constructing phonon computers, electronic-inspired computation has also impacted how information is encoded. Prior efforts encoded information in temperature differences. But when phonons alone are information carriers, one could take inspiration from optical computing, encoding information in the polarization of the phonon current. Logical 1 (0) would be vertically (horizontally) polarized transverse phonons. Logic operations in this computer therefore correspond to modifying the polarization of phonon currents. Kittel first realized the possibility of controlling phonon polarization. He discovered the acoustic Faraday effect (AFE, or acoustic Faraday rotation, it rotates the angle of polarization) for ultrasonic waves in ferromagnets subject to a uniform magnetic field [12]. Interest in this application seems to have ended there. Instead, the focus on magneto-acoustic (MA, also called magneto-elastic) effects (the influence of a magnetic field on phonons) has been to discover new mechanisms for MA effects and how they might aid in characterizing materials [13–15] or controlling magnons [16].

Here we consider the construction of logic from MA ma-

Electronic Computing



Phonon Computing

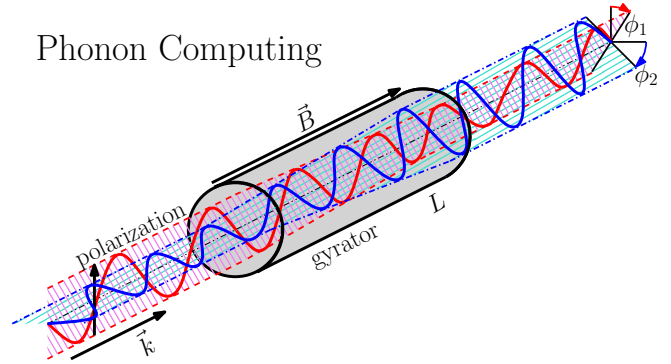


FIG. 1: (COLOR ONLINE) Comparing electronic and phononic computing. Electronic computing uses a stream of electrons through a solid-state transistor to control the magnitude of the voltage at the drain. Conversely, our implementation of phonon computing has transverse phonons undergo an acoustic Faraday rotation, controlling the polarization of the transmitted signal. Note the use two incident phonon currents with different polarizations and frequencies, each rotated by a different angle while traversing the gyrator.

terials beginning with the fundamentals - sources, wires, and operators. Attention will be paid to gyrators, where we find that, in addition to isolators (the optical analog of diodes), gyrators can create transistors. Logic gates are constructed from these transistors. We analyze how individual gates could perform a new form of parallel computing (which we term rainbow parallelization, RP) (Figure 1).

It is helpful to consider where a signal comes from and how it reaches computing elements. Waste heat would be the ideal source of cheap, convenient phonons, but it lacks

coherence, intensity, and polarization. At the other extreme, the phonon laser [17] has good beam characteristics but is in the early stages of development. For MA, acoustic transducers are a promising compromise. Piezoelectrics (e.g. AC-cut quartz) convert electronic signals into polarized phonons currents, with polarization depending on the crystallographic plane at the interface [18]. At higher frequencies (GHz to THz, instead of MHz to GHz), femtosecond lasers can be transduced into picosecond phonon pulses via thin metallic films (e.g. polycrystalline Al on Zn) [19, 20]. Once phonons have been produced, they can be steered via wires. Any material with good lattice thermal conductivity would do, as this implies that phonons propagate quickly and retain polarization over long distances (long phonon mean free path).

While the previous elements are similar to their electrical counterparts, operators are not. In digital electronics, operators (e.g. transistors) control voltage levels (logic states) by blocking or admitting electrical current; whereas operators in polarization-based computing always admit currents (states are modified by switching polarizations). Given our basis, a change of state is accomplished by having a gyrator rotate the polarization by $\pi/2$. Gyrators can be constructed from any material possessing the AFE (e.g. MA) (Figure 1). In the AFE, a longitudinal magnetic field ($\vec{B} \parallel \vec{k}$, \vec{k} is the phonon wave-vector) induces circular birefringence (two circularly polarized modes travel at different speeds). Every linearly polarized mode is composed of a superposition of circularly polarized modes, which reach the end of the gyrator at different times. This phase difference between the circular modes yields a linearly polarized current with a new polarization. The magnetic field strength determines the magnitude of the gyration [21]. There are many MA materials known [13], although yttrium iron garnet (YIG) is a good candidate here as the AFE has been observed at room temperature [21].

Currently, when gyrators are used, they are paired with a fixed magnet (often 0.01-10T) to give a predefined gyration. This design has some uses in computing (e.g. when creating isolators), but gyrators have other uses. We propose that a phonon current could control the strength of the magnetic field, allowing the gyrators to operate in a completely new way. One control mechanism is to transduce a second current, rectifying and amplifying the resultant signal, and using this signal to allow or block a fixed current from reaching an electromagnet (Figure S1). With this sort of controlled magnetic field, gyrators become three terminal devices that act like generalized transistors. Signals propagate from one side of the gyrator to the other (source to drain), but the gating current on the magnet controls the outgoing polarization. Importantly, treating the gate as the input and the drain as the output, the signal is amplified (as in electronic transistors). This is an advantage over isolator-based designs (e.g. some forms of optical computing [22]), as losses accumulate and hinder detection.

With these transistors, we can construct basic logic gates. First, consider a NOT gate. Given our basis, the easiest implementation is a $\pi/2$ gyrator (0 in gives 1 out, 1 in gives -0 out. To remove the negative sign, which is an overall phase, the output can be fed into the source and gate of a π gyrator,

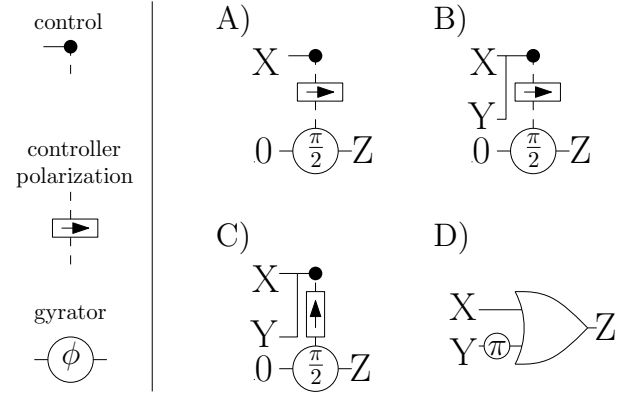


FIG. 2: Implementing transistor logic with phonon gyrators. Elements are defined in sidebar. X and Y are inputs, Z is output, and 0 is an input fixed to logical 0. (a) NOT gate (b) NAND gate (c) OR gate (d) coherent XOR gate (using OR).

the gyrator activated by 0). This design is good for changing OR/NOR and AND/NAND, but an amplifying design is straightforward (Figure 2(a)). Logical 0 is fed into the source of a gyrator and the signal to be inverted is applied at the gate. Logical 0 at the gate activates the gyrator, rotating the source signal by $\pi/2$, yielding logical 1 at the drain. However, logical 1 at the gate does not trigger the control, so the gyrator is not activated and the drain is at logical 0. Now consider two signals at the gate (Figure 2(b)). When the phonons are in a definite polarization, two signals will superimpose (no polarization change for identical inputs and $\pm\pi/4$ polarization for orthogonal signals). Control activates when this total signal has a horizontally polarized component greater than a critical value. Thus, if either input is logical 0, then control will activate and the output will be logical 1. Only when both inputs are vertical will the output be logical 0. Therefore, this circuit is NAND. Control could alternatively select logical 1 (Figure 2(c)). Now, the output will only be logical 0 when both inputs are as well, ergo this circuit is OR. With either NAND/OR and NOT, we can use De Morgan's laws to create any logic gate. But for coherent phonons, XOR is simple (Figure 2(d)). Essentially, there is now destructive interference in the OR gate for signals of identical polarization, so the current can only exceed the critical amplitude when the signals are orthogonal. And since a $\pm\pi/4$ polarized signal activates control, this OR gate is now an XOR.

While these designs are quite simple, there are other realizations of logic gates. Exploiting De Morgan's laws, we can construct any operation using only $\pi/2$ gyrations and vertical control elements (Figure S2). Using gates in fixed arrangement and selectively (de)activating them, we can perform arbitrary operations (as in an FPGA). From this, single circuit parallel computing (RP) follows. Consider multiple signals of different frequencies all entering the same generic circuit. Independently controlling which gyrators and control elements work at which frequency, we can independently select the logical operation for each frequency. Such control is feasible with multistage gyrators (Figure 3) – several gyrators in series where the sum of the gyrations at a given frequency is

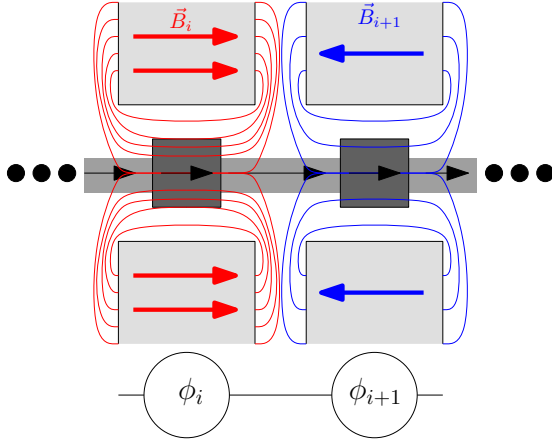


FIG. 3: (COLOR ONLINE) Multistage gyration: a concatenation of several gyrators. The lengths and magnetic field strengths at each stage are tuned to control the gyrations at multiple frequencies.

equal to the desired gyration

$$\Phi(\omega_i) = \sum_{(j)} L_{(j)} \phi(\omega_i, B_{(j)}) \quad (1)$$

$B_{(j)}$ is the magnetic field strength of the j^{th} stage, $L_{(j)}$ its length, ω_i the frequency of the i^{th} input, $\Phi(\omega_i)$ its gyration, and ϕ the gyration per unit length. The number of stages required for a multistage gyration scales as $O(N)$ for ungated elements and $O(N^\alpha)$ ($\alpha \in [1, 2]$ and depends upon the design used) for gated elements. These scalings can be improved by combining stages (allowing fringing fields to come to bear, slightly complicating the design and discussed in the supplementary materials). Control of different frequencies can be accomplished by filtering signals before amplification.

Assuming uniform magnetic field, the polarization shifts obey Eq.1, one can easily find $L_{(i)}(\{B\}, \{\Phi\}, \{\omega\})$ by inverting $\phi(\omega_i, B_{(j)})$ ($\{\}$ denote sets). The exception to this is when the $\phi(\omega_i, B_{(j)})$ is separable ($\phi = f(\omega)g(B)$). While this is not generically the case with phonons, it is for optics (where $\phi = V(\omega)B$) [23], the exceptions principally due to absorption (often in cold gases [24]). RP is (to our knowledge) presently unique to phonons (voltage is scalar, so manipulating polarization is impossible in classical digital circuits), at least at room temperature. To show the feasibility of this type of design for phonons, we calculate $L_{(i)}(\{B\}, \{\Phi\}, \{\omega\})$ for a 2-frequency, 2-stage gyration with no gyration induced at the lower frequency and a $\pi/2$ gyration induced at the higher frequency. The gyration $\Phi(\omega; \{B\}, \{L\})$ for the multistage gyration is plotted in Figure 4. $\text{Im}[\Phi] < 0$ denotes absorbance. Waveforms at the two frequencies are found analytically in

real space (Figure 4 insets). The higher frequency mode has almost no loss ($< 10^{-6}\%$), while the lower has a loss of 19.8%. Finally, consider the number of stages possible for a given frequency and magnetic field strength range. We calculate (see supplementary materials) the maximum number of channels currently accessible is about 2700. Such a large number of channels is principally due to the large Q factor of

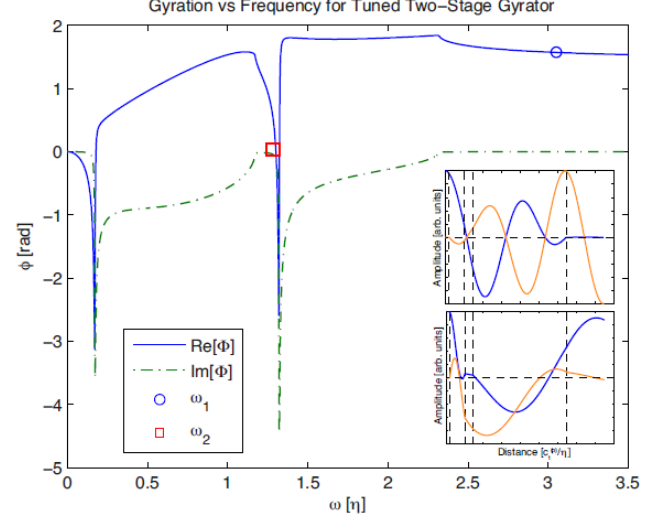


FIG. 4: (COLOR ONLINE) Rainbow Parallelization: designing a 2-stage gyration to work at two frequencies. Total gyration as a function of frequency plotted in blue. Absorption ($\text{Im}[\Phi]$) in dashed green. Circled frequencies have $\Phi = 0$ and $\Phi = \pi/2$. ω is rescaled by η (the MA coupling rate). (inset) Real space representation of the waveforms for the two selected frequencies selected. L is rescaled by $c_t^{(p)}/\eta$ ($c_t^{(p)}$ is the transverse phonon speed). Bottom/top figure is for lower/higher frequency mode with blue (orange) denoting horizontal (vertical) polarization. Vertical lines denote boundaries (2nd and 4th intervals are gyrators).

YIG, which makes it possible to distinguish very small frequency separations.

We have demonstrated a new mode of operation of an acoustic gyration and used it to create basic logic gates. By exploiting the wave nature of phonons and the tunable nonlinearity of MA, we demonstrate that MA materials can perform RP, an effect that is presently unique to this computing architecture. This suggests that there might be circumstances where a phonon computer could outperform an electronic computer.

This material is based upon work supported by the National Science Foundation Graduate Research Fellowship under Grant No. 1122374. Supporting data and figures relevant to this work are presented online under supplementary materials.

[1] L. Grover, in *Proceedings of the twenty-eighth annual ACM symposium on Theory of Computing* (ACM, New York, NY, USA, 1996) p. 212-219.

[2] L. M. Adelman, *Science* **266**, 1021–1024 (1994).

[3] A. Robinson, *Nature* **463**, 736 (2010).

[4] N. Li, J. Ren, L. Wang, G. Zhang, P. Hänggi, and B. Li, *Rev.*

- Mod. Phys.* **84**, 1045-1066 (2012).
- [5] L. Wang and B. Li, *Phys. Rev. Lett.* **99**, 177208 (2007).
 - [6] B. Li, L. Wang, and G. Casati, *Phys. Rev. Lett.* **93**, 184301 (2004).
 - [7] W.C. Lo, L. Wang, and B. Li, *J. Phys. Soc. Japan* **77**, 054402 (2008).
 - [8] L. Wang and B. Li, *Phys. Rev. Lett.* **101**, 267203 (2008).
 - [9] C. Chang, D. Okawa, A. Majumdar, and A. Zettl, *Science* **314**, 1121 (2006).
 - [10] R.-G. Xie, C.-T. Bui, B. Varghese, M.-G. Xia, Q.-X. Zhang, C.-H. Sow, B. Li, and J.T.L. Thong, *Adv. Funct. Mater.* **21**, 1602 (2011).
 - [11] M. Terraneo, M. Peyrard, and G. Casati, *Phys. Rev. Lett.* **88**, 094302 (2002).
 - [12] C. Kittel, *Phys. Rev.* **110**, 836 (1958).
 - [13] J.D. Gavenda, V.V. Gudkov, *Magnetoacoustic Polarization Phenomena in Solids* (Springer, New York, NY, 2000).
 - [14] M. Boiteux, P. Doussineau, B. Ferry, J. Joffrin, and A. Levelut, *Phys. Rev. B* **4**, 3077 (1971).
 - [15] A. Sytcheva, U. Löw, S. Yasin, J. Wosnitza, S. Zherlitsyn, P. Thalmeier, T. Goto, P. Wyder, and B. Lüthi, *Phys. Rev. B* **81**, 214415 (2010).
 - [16] M. Bombeck *et al.*, *Phys. Rev. B* **85**, 195324 (2012).
 - [17] K. Vahala, M. Herrmann, S. Knz, V. Batteiger, G. Saathoff, T. W. Hänsch, and T. Udem, *Nat. Phys.* **5**, 682 - 686 (2009).
 - [18] B. Lüthi, *Physical Acoustics in the Solid State* (Springer, New York, NY, 2007).
 - [19] D. Hurley, O.B. Wright, O. Matsudaa, V.E. Gusevc, and O.V. Kolosov, *Ultrasonics* **38**, 470 (2000).
 - [20] O. Matsuda, O. B. Wright, D. H. Hurley, V. E. Gusev, and K. Shimizu, *Phys. Rev. Lett.* **93**, 095501 (2004).
 - [21] H. Matthews and R.C. LeCraw, *Phys. Rev. Lett.* **8**, 397 (1962).
 - [22] J. Ballato and E. Snitzer, *Appl. Opt.* **34**, 6848-6854 (1995).
 - [23] A.K. Zvezdin and V.A. Kotov, *Modern Magneto-optics and Magneto-optical Materials*, (CRC Press, New York, NY, 1997).
 - [24] D. Budker, W. Gawlik, D. F. Kimball, S. M. Rochester, V. V. Yashchuk, and A. Weis, *Rev. Mod. Phys.* **74**, 1153 (2002).

Beyond electronics, beyond optics: single circuit parallel computing with phonons

Supplementary Material

Sophia Sklan¹ and Jeffrey C. Grossman²

¹*Department of Physics, Massachusetts Institute of Technology, Cambridge, Massachusetts, 02139, United States.*

²*Department of Materials Science and Engineering, Massachusetts Institute of Technology, Cambridge, Massachusetts, 02139, United States.*

I. CLASSES OF MAGNETO-ACOUSTIC MATERIALS

There are several criteria for a material to be able to support the magnetoacoustic interactions necessary for the acoustic Faraday effect [13]. First, it must be a crystalline material with at least C_3 (3-fold rotation) symmetry. Second, there must be some intermediate field to couple the phonon modes to the magnetic field. This is necessary because the Lorentz force acting on a phonon is generally negligible. The intermediate field can be photons, electronic charge, or magnons. For photon-phonon coupling, the relevant interactions arise in low temperature metals, where a magnetic field allows the propagation of helicon (for uncompensated metals) and doppleron or Alfvén wave (for both compensated and uncompensated metals) modes. These modes have been studied in pure metals (copper, nickel, etc), where it is found that dopplerons (which have phase and group velocities antiparallel to each other) are only supported for very small sets of wavevectors.

In electron-phonon coupling, the relevant interaction is a coupling between the octupole moment of the 3d (as in CeAl₂), 4f (as in TGG), or higher order charge distributions and the crystalline electric field (CEF). These interactions arise because the nuclei in the crystal are charged, and so distortions of the lattice will induce distortions of the electronic structure and vice versa. For materials of high rotational symmetry, the lower order modes of the charge distribution (monopole, dipole, quadrupole) are less significant. Because these materials have multiple phonon bands (i.e. acoustic and optical branches), [15, 25] found that they have two types of magnetoacoustic interactions. In addition to the typical coupling scheme (magnetic field to electronic charge to crystalline field to phonons) there is also an indirect coupling, where magnetoelastic effects in one branch can induce them in other branches due to phonon-phonon couplings. Additionally, there is a second class of electron-phonon interactions capable of supporting magnetoacoustic effects. This is doppler-shifted cyclotron resonance (DSCR), which occurs under similar circumstances to helicon-phonon and doppleron-phonon couplings (i.e. low temperature pure metals).

Lastly, in magnon-phonon coupling, the dependence of the exchange interactions in the spin Hamiltonian upon the location of the nuclei implies a dependence of the magnon bands upon the vibrational distortion of the lattice. This is essentially an ionic magnetostriction effect. It is found in both ferromagnets (for example YIG [12]), antiferromagnets or flopped antiferromagnets (as in Cr₂O₃ [14]), or paramagnets doped with magnetic impurities (single molecule magnets, as in KMgF₃+Ni [26]). It is an open question if phonon-phonon effects can induce a second type of magnetoacoustic

interaction for magnon-phonon coupling schemes (the conclusions that we draw here still work qualitatively if these effects are present, but the quantitative description would need to be modified). Since the acoustic Faraday effect is most extensively studied at room temperature in magnon-phonon coupling schemes (in particular in YIG), we shall YIG for our magnetoacoustic element.

II. CONTROL MECHANISMS

There are two basic classes of magnetic control. Control can either be direct or indirect. In direct control, the magnetic field is modified by the phonon current itself, and in indirect control the phonon current transduces some intermediate signal which can control the magnetic field. Direct control can be performed by a ferromagnet (see Fig. S1(a)). When a phonon current is incident upon the magnet, a portion can be absorbed or converted into localized modes that heat up the magnet. This increase in temperature will result in increased disorder of the magnetization within the crystal, forming domains and weakening the total magnetization. Since the spontaneous magnetization is temperature dependent, the resultant magnetic field will be modified after a negligible delay (since changes in field propagate at the speed of light). If the temperature achieved is never so great as to demagnetize the entire magnet, there will be always be a net magnetization in a fixed direction, which means that upon cooling the down the direction of the total magnetization will remain fixed (thus keeping our gyrators acting like gyrators and not polarizers). While this approach is clearly the simplest to engineer, there are some limitations to direct control. First, if the thermal conductivity and specific heat of the magnet are not (approximately) linear within the range of temperatures achieved, then it is exceedingly difficult to control the strength of the magnetic field. What's more, the heating of the magnet depends upon the total thermal current, rather than any particular polarization or frequency. While polarizers can eliminate transverse polarizations (and even frequency intervals, when pairs of orthogonal polarizers are used), there is no easy way to eliminate the longitudinal modes. While we can normally safely ignore these modes (as in every other element, they are completely decoupled), here controlled operation would require us to either account for or eliminate any longitudinal effects. Lastly, because the phonons are being converted into magnetic disorder, they are being destroyed in this process and cannot be used in other circuit elements.

Indirect control gets around many of these disadvantages. In the control scheme given here, there are three stages (Fig. S1(b), stages shown in insets). First, the phonon current is sent

through a piezoelectric material (or some other linear, polarization sensitive transducer). The piezoelectric is cut such that the faces of the crystal correspond to the polarization vectors of the basis of transverse modes. The transverse modes will distort the crystal, inducing a fluctuating electrization which will produce an oscillating voltage gradient. This voltage gradient will be directed parallel to the polarization vector of the phonon current and have magnitude linearly dependent upon the phonon amplitude, that is $\partial_i V \propto \epsilon_{iz}$ (where ϵ_{iz} is the strain component in the i th direction of a mode propagating along z). Placing wires at the faces of piezoelectric will result in a very small AC voltage that depends solely upon a given phonon mode (i.e. $\Delta V \propto \hat{n}_i \epsilon_{iz}$, where \hat{n} is the normal vector of the crystal surface). Because the energy extracted is so small, the phonon current leaves the piezoelectric essentially without loss. At the second stage, this voltage is converted into a finite, constant voltage (removing all non-transient time dependence is necessary to keep the magnetic field from fluctuating). This conversion is accomplished by using a concatenation of voltage multiplying rectifiers. The number of rectifiers used will increase the output voltage at this stage, so arbitrary voltages can be achieved in principle. This voltage could be used to drive the current in an electromagnet (stage three), which would give a magnetic field that is approximately linear in the amplitude of a polarized phonon current (linearity is maintained so long as the total magnetic field remains well below the maximum possible). Strict linearity, however, can be a drawback in building digital circuits. For example, in the construction of an OR gate it is preferable to have signals of strength ϵ and 2ϵ give identical fields (corresponding to inputs of $X=1, Y=0$ and $X=1, Y=1$, respectively). To achieve this sort of digital control, the voltage produced at the end of stage two is used to control the gate of an electronic transistor (see Fig. S1(c)). Since the current produced is the one that flows from source to drain, the transistor output is (approximately) a digital response to the gate voltage. The amplitude dependence of these three types of control regimes is summarized in Fig. S1(d). Since large magnetic fields are typically required to achieve strong magnetoacoustic effects (typically in the range of .5 to 10 T [14, 21], sometimes fields of up to 20 T have been used [15]), the electromagnet will have to be quite powerful. Bitter electromagnets, for example, have been constructed to produce continuous fields of at least 35 T (superconducting magnets can exceed this, but not at room temperature) [27], far higher than any the fields required by our system.

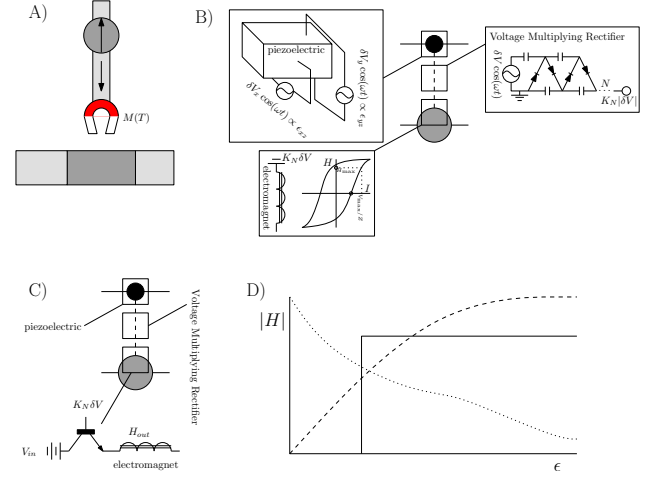


FIG S1: Magnetic control designs. (a) Direct control by phonons. (b) Linear indirect control. (c) Digital indirect control. (d) Magnetic field as a function of amplitude. The dotted line denotes direct control. The dashed line denotes linear indirect control. The solid line denotes digital indirect control.

III. SIMILARITY OF LOGIC GATES

To determine the minimum number of gates required to construct all the two-terminal logic functions, we specialize to only using $\pi/2$ gyrations and vertical control. By explicit construction (see Fig. S2), we see that we require three control elements (one for each input, one for their superposition), and seven gyrators (three controlled, four fixed). Given that control elements are always paired to gyrators, this gives a total of seven elements to perform all sixteen logic operations.

X Y 0 0	X Y 0 0	X Y 0 0	X Y 0 0
0	XY	XY	X
X Y 0 0	X Y 0 0	X Y 0 0	X Y 0 0
XY	Y	$X \oplus Y$	$X + Y$
X Y 0 0	X Y 0 0	X Y 0 0	X Y 0 0
XY	$X \oplus Y$	\bar{Y}	$X + \bar{Y}$
X Y 0 0	X Y 0 0	X Y 0 0	X Y 0 0
\bar{X}	$\bar{X} + Y$	$\bar{X} + \bar{Y}$	1

FIG S2: Alternative transistor logic using only vertical control and 90 degree gyrations. Implementations of all 16 two-terminal logic functions.

IV. INCORPORATION OF INHOMOGENEITY INTO MULTI-STAGE GYRATOR DESIGN

The Faraday rotation induced by a uniform magnetic field is straightforward to calculate. When the magnetoacoustic inter-

action is due to magnon-phonon resonance, it takes the form

$$\begin{aligned}\Phi &= \int dz \frac{k_+ - k_-}{2} \\ &\approx V \int dz \frac{\omega^2}{\omega^2 - \Omega^2} \\ &= L\phi\end{aligned}$$

where Φ is the total rotation, V is a constant (the analog of the Verdet constant), ω the phonon frequency, Ω the effective magnon frequency, z the runs over the thickness of the gyrator along the direction of propagation (L), and ϕ is the gyration per unit length [13]. In a strong, uniform magnetic field ($\vec{B} \equiv B\hat{z}$), $\hbar\Omega \approx \gamma|B|$, where γ is the gyro-magnetic ratio ($g_s\mu_B$ for spins). When the magnetic field is not uniform (which can occur for multistage gyrators), calculating the Faraday modes is more complicated. We assume a gradual inhomogeneity (that is, only including the effects of varying the magnon modes themselves, ignoring the deviation of the coupled mode Hamiltonian from the Faraday regime). Consider the inhomogeneous magnetic field $B = -\frac{1}{2}B'(z)(\vec{x} + \vec{y}) + B(z)\hat{z}$, where $B'(z) = \frac{dB(z)}{dz} \ll B(z)$ and the term proportional to the derivative of the field is necessary to satisfy $\nabla \cdot B = 0$. This gives a vector potential $A = -\frac{1}{2}B(z)(y\hat{x} - x\hat{y})$, thereby maintaining the orbital Zeeman term proportional to $B(z)L_z$. The spin Zeeman term, which is more important in this context, is proportional to $B \cdot S$. The electronic degrees of freedom will arrange themselves properly so that $B(z)S_z$ can be evaluated unambiguously at fixed z , i.e. that $\omega_{nq}^{(m)} \rightarrow \omega_{nq}^{(m)(0)}(z)$, ($\omega_{nq}^{(m)(0)}$ is the magnon frequency for the n th branch/polarization and wavevector q , calculated to 0th order in transverse component) which can be integrated over in determining the Faraday rotation. The terms perpendicular to \hat{z} , on the other hand, will perturb the magnon Hamiltonian, shifting the frequencies. We treat these additional terms as a perturbation upon $\omega_{nq}^{(m)}(z)$, keeping terms less than $O(\alpha^3)$, as we did in our previous derivation. The perturbation Hamiltonian, in Holstein-Primakoff coordinates is:

$$\Sigma_q B'(z) \sqrt{2S} [x^-(q)\alpha(q) + x^+(-q)\alpha^\dagger(q)]$$

where

$$\begin{aligned}x^\pm(q) &= -i\left[\frac{\partial}{\partial q_x} \pm i\frac{\partial}{\partial q_y}\right] \\ &= -i\sqrt{\frac{3}{8\pi}} \mathcal{F}[rY_1^{\mp 1}(\hat{r})]\end{aligned}$$

(\mathcal{F} is the Fourier transform operator, r is distance, and Y_l^m are the spherical harmonics), which (to lowest order) can be considered a constant so far as spin degrees of freedom are concerned. The first order correction vanishes trivially, and the second order is

$$\frac{2S[B'(z)]^2}{\hbar^2\omega_{nq}^{(m)(0)}(z)} [|\langle x_{-q}^- \rangle|^2 - |\langle x_{-q}^+ \rangle|^2],$$

which is generically nonzero.

V. DESIGN OF A MULTISTAGE GYRATOR

While the use of inhomogeneous magnetic fields makes for a more elegant form of single circuit parallelization (in principle, only a single magnetoacoustic material is required, with the magnetic field programmable by a set of control elements), it does make design more difficult. For uniform fields, the relation

$$\Phi(\omega_i) = \sum_{(j)} L_{(j)} \phi(\omega_i, B_{(j)})$$

is clearly satisfied, meaning that we can invert the ϕ matrix to determine the necessary length. To demonstrate how this design works, we consider the problem of designing a two frequency circuit which flips one mode and passes the other. To calculate the exact Faraday rotation we use $k_\pm^2 = k_0^2(1 + \frac{\eta}{\omega_s \pm \omega - \eta})$ where $c_t^{(p)}k_0 = \omega$ ($c_t^{(p)}$ is the transverse speed of sound), ω_s the magnon frequency, and $\hbar\eta = 4|G_{44}|^2 S^3/M$ is magnetoelastic coupling energy (G_{44} is the coupling constant, S is spin, and M is the effective mass). The Faraday rotation equation given previously is based upon the assumption that $k_+ - k_- = (k_+^2 - k_-^2)/2k_0$ (i.e. $k_+ + k_- \approx 2k_0$). While this approximation is generally useful, it does not give an easy way to calculate the absorption of the incident wave.

We work in units such that the equations simplify, i.e. $\Omega \equiv \omega_s - \eta \approx \gamma B - \eta + i\Gamma \equiv B + i\Gamma$, and rescale all the variables ($\omega \rightarrow \omega/\eta$, $B \rightarrow B/\eta$, $\Gamma \rightarrow \Gamma/\eta$, $k \rightarrow c_t^{(p)}k/\eta$, $L \rightarrow \eta L/c_t^{(p)}$, $\phi \rightarrow \phi$) giving the relation $k_\pm^2 = \omega^2(1 + \frac{1}{B \pm i\Gamma \pm \omega})$. For clarity, we keep the magnon lifetime ($\tau_s = 1/\Gamma$) long, setting $\Gamma = 0.0023$. We select $B_1 = 1.32$ and $B_2 = 0.17$, thus making it unlikely that our values happen to simplify the problem (we also want the magnetic field values reasonably well separated, as significant losses appear in the range $\text{Re}[\omega] = [B, B + 1]$). For $\Phi_2 = \pi/2$, it is best to select a frequency far from resonance, so we set $\omega_1 = 3.05$. To make $\Phi_1 = 0$, it is necessary for it to be close to resonance with a magnon mode (this is implied by the shape of the Faraday rotation curve). Thus, $\omega_2^2 = 1.3^2 - \Gamma^2$. Solving for the lengths then gives $L_1 = 0.403$ and $L_2 = 2.51$. A plot of the total gyration as a function of frequency quickly confirms that this device acts as predicted. To translate this plot into the real space wavefunction, we assume impedance matching at the boundaries (i.e. ignoring losses due to reflection). This allows us to isolate the losses due to the finite lifetime, which we find to be $3.81 \times 10^{-7}\%$ at ω_1 and 19.8% at ω_2 .

VI. THE MAXIMUM NUMBER OF CHANNELS CURRENTLY ACCESSIBLE

The number of possible channels for a multi-stage gyrator is difficult to determine. In principle, an infinite number of stages could support an infinite number of channels, but since the complexity of the device increases as the number of stages increases. Moreover, there are limitations to the frequencies and field strengths that are feasible. As such, only a small subset of the channels physically accessible. Since the strength of

the magnetic field can be controlled experimentally so long as the electromagnets used are below their saturation magnetization, we are limited more by the resolution of phonon modes. We estimate the spectral resolution of the phonon modes using the Q-factor. To make sure that the frequencies are distinguishable, we assume $\omega_N + \frac{1}{2}\Delta\omega_N = \omega_{N+1} - \frac{1}{2}\Delta\omega_{N+1}$ where ω_N is the Nth frequency used and $\Delta\omega$ is the bandwidth. Essentially, this relation implies that frequencies are separated by their average bandwidth. Plugging in the definition of $Q_N = \omega_N / \Delta\omega_N$, we find that

$$\omega_N / \omega_0 = \prod_{n=0}^N \frac{2Q_n + 1}{2Q_n - 1} \leq \left(\frac{2Q_{\min} + 1}{2Q_{\min} - 1} \right)^N.$$

Therefore

$$N \geq \ln\left(\frac{\omega_N}{\omega_0}\right) / \ln\left(\frac{2Q_{\min} + 1}{2Q_{\min} - 1}\right) \approx Q_{\min} \ln \frac{\omega_N}{\omega_0}$$

(the error in this approximation is <1% for $Q > 10$). Setting $\omega_N = \omega_{\max}$, $\omega_0 = \omega_{\min}$ gives the number of distinguishable

frequencies accessible. Experimentally, the majority of MA experiments concentrate in the range $\omega/2\pi \in 10\text{MHz}$ to GHz [13]. For magnetic fields of $\leq 10\text{T}$, however, the cyclotron frequency (i.e. the magnon frequency) is 152 MHz. We therefore lack the ability to easily tune gyrations above this frequency. Q for YIG is typically quite large in this frequency, values between 10^4 and 10^7 are regularly found for frequencies between 10MHz and 1GHz ($Q \propto 1/\omega$) [28]. However, when the intensity of the phonon current is too great (1mW is the rule of thumb in the 500MHz-1GHz range), the magnon coupling is no longer linear and the Q factor degrades (the phonons lose energy to magnons, which quickly decay). This degradation is typically of order unity, but we shall take a conservative estimate of Q as 10^3 . This gives $N = 2700$. This could be improved even further by countering the reduction of the Q factor, as well as extending the range of accessible frequencies. Conversely, given that this many channels would make fabrication dramatically more complicated, the a portion of the channels could be sacrificed (e.g. reducing the maximum strength magnetic field to a more readily achievable value).

-
- [1] L. Grover, in *Proceedings of the twenty-eighth annual ACM symposium on Theory of Computing* (ACM, New York, NY, USA, 1996) p. 212-219.
 - [2] L. M. Adelman, *Science* **266**, 1021–1024 (1994).
 - [3] A. Robinson, *Nature* **463**, 736 (2010).
 - [4] N. Li, J. Ren, L. Wang, G. Zhang, P. Hänggi, and B. Li, *Rev. Mod. Phys.* **84**, 1045-1066 (2012).
 - [5] L. Wang and B. Li, *Phys. Rev. Lett.* **99**, 177208 (2007).
 - [6] B. Li, L. Wang, and G. Casati, *Phys. Rev. Lett.* **93**, 184301 (2004).
 - [7] W.C. Lo, L. Wang, and B. Li, *J. Phys. Soc. Japan* **77**, 054402 (2008).
 - [8] L. Wang and B. Li, *Phys. Rev. Lett.* **101**, 267203 (2008).
 - [9] C. Chang, D. Okawa, A. Majumdar, and A. Zettl, *Science* **314**, 1121 (2006).
 - [10] R.-G. Xie, C.-T. Bui, B. Varghese, M.-G. Xia, Q.-X. Zhang, C.-H. Sow, B. Li, and J.T.L. Thong, *Adv. Funct. Mater.* **21**, 1602 (2011).
 - [11] M. Terraneo, M. Peyrard, and G. Casati, *Phys. Rev. Lett.* **88**, 094302 (2002).
 - [12] C. Kittel, *Phys. Rev.* **110**, 836 (1958).
 - [13] J.D. Gavenda, V.V. Gudkov, *Magnetoacoustic Polarization Phenomena in Solids* (Springer, New York, NY, 2000).
 - [14] M. Boiteux, P. Doussineau, B. Ferry, J. Joffrin, and A. Levelut, *Phys. Rev. B* **4**, 3077 (1971).
 - [15] A. Sytcheva, U. Löw, S. Yasin, J. Wosnitza, S. Zherlitsyn, P. Thalmeier, T. Goto, P. Wyder, and B. Lüthi, *Phys. Rev. B* **81**, 214415 (2010).
 - [16] M. Bombeck *et. al.*, *Phys. Rev. B* **85**, 195324 (2012).
 - [17] K. Vahala, M. Herrmann, S. Knzn, V. Batteiger, G. Saathoff, T. W. Hänsch, and T. Udem, *Nat. Phys.* **5**, 682 - 686 (2009).
 - [18] B. Lüthi, *Physical Acoustics in the Solid State* (Springer, New York, NY, 2007).
 - [19] D. Hurley, O.B. Wright, O. Matsudaa, V.E. Gusevc, and O.V. Kolosov, *Ultrasonics* **38**, 470 (2000).
 - [20] O. Matsuda, O. B. Wright, D. H. Hurley, V. E. Gusev, and K. Shimizu, *Phys. Rev. Lett.* **93**, 095501 (2004).
 - [21] H. Matthews and R.C. LeCraw, *Phys. Rev. Lett.* **8**, 397 (1962).
 - [22] J. Ballato and E. Snitzer, *Appl. Opt.* **34**, 6848-6854 (1995).
 - [23] A.K. Zvezdin and V.A. Kotov, *Modern Magneto-optics and Magneto-optical Materials*, (CRC Press, New York, NY, 1997).
 - [24] D. Budker, W. Gawlik, D. F. Kimball, S. M. Rochester, V. V. Yashchuk, and A. Weis, *Rev. Mod. Phys.* **74**, 1153 (2002).
 - [25] P. Thalmeier, *Phys. Rev. B* **80**, 214421 (2009).
 - [26] J.W. Tucker, *J. Phys. C: Solid State Phys.* **13**, 1767 (1980).
 - [27] S. Hannah and E. Palm, *J. Low Temp. Phys.* **159**, 366 (2010).
 - [28] R.C. LeCraw and R.L. Comstock, in *Physical Acoustics: Principles and Methods*, edited by W.P. Mason (Academic Press, New York, 1964), vol. 3B, p. 127.